Segmentation of Human Aorta Using 3D nnU-Net-Oriented Deep Learning

Feng Li,[1,2] Lianzhong Sun,[1] Kwok-Yan Lam,[2] Songbo Zhang,[1] Zhongming Sun,[1] Bao Peng,[3] Hongzeng Xu,[4,5,a)] and Libo Zhang[5]

[1)]*Zhejiang Gongshang University, Hangzhou, 310018, China.*

[2)]*Nanyang Technological University, 639798, Singapore.*

[3)]*Shenzhen Institute of Information Technology, Shenzhen, 518172, China.*

[4)]*The People's Hospital of China Medical University, The People's Hospital of Liaoning Province, No. 33, Wenyi road, Shenhe District, Shenyang City, Liaoning Province, 110011, China.*

[5)]*Key Laboratory of Cardiovascular Imaging and Research of Liaoning Province, Shenyang, 110016, China.*

(Dated: 26 May 2023)

Computed tomography angiography (CTA) has become the main imaging technique for cardiovascular diseases. Before performing the transcatheter aortic valve intervention (TAVI) operation, segmenting images of the aortic sinus and nearby cardiovascular tissue from enhanced images of the human heart is essential for auxiliary diagnosis and guiding doctors to make treatment plans. This paper proposes a nnU-Net (no-new-Net) framework based on deep learning (DL) methods to segment the aorta and the heart tissue near the aortic valve in cardiac CTA images, and verifies its accuracy and effectiveness. Total 130 sets of cardiac CTA image data (88 training sets, 22 validation sets and 20 test sets) of different subjects have been used for the study. The advantage of the nnU-Net model is that it can automatically perform preprocessing and data augmentation according to the input image data, can dynamically adjust the network structure and parameter configuration, and has a high model generalization ability. Experimental results show that the DL method based on nnU-Net can accurately and effectively complete the segmentation task of cardiac aorta and cardiac tissue near the root on the cardiac CTA dataset, and achieve an average Dice similarity coefficient (DSC) of 0.9698 ± 0.0081. The actual inference segmentation effect basically meets the preoperative needs of the clinic. Using the DL method based on the nnU-Net model solves the problems of low accuracy in threshold segmentation, bad segmentation of organs with fuzzy edges, and poor adaptability to different patients' cardiac CTA images. nnU-Net will become an excellent DL technology in cardiac CTA image segmentation tasks.

Computer preoperative simulation and preoperative evaluation have great significance in the process of transcatheter aortic valve intervention (TAVI). The segmentation and extraction of the aorta based on cardiac computed tomography angiography (CTA) images is an important basic work in TAVI operation simulation. To date, a variety of calculation methods have been proposed to segment cardiac CTA images. These methods can be roughly divided into traditional methods and DL methods. Traditional methods include the 3D hierarchical region growing algorithm[1], morphological method[2], combination of Hough transform and region growing algorithm[3], active contour model algorithm[45], and suitable shape variability model based on piecewise affine degrees of freedom[6]. Generally, the traditional cardiac segmentation method has a faster speed, but the segmentation results of traditional algorithms are easily affected by problems such as image contrast quality and other cardiac tissue interference. The segmentation accuracy of traditional methods is often poor when used for cardiac CTA images of a variety of subjects, and thus, these methods are not widely used in clinical practice.

In recent years, the rapid development of deep learning (DL) has greatly promoted the process of cardiac CTA segmentation, and an increasing number of DL methods have shown better performance than traditional methods. Cardiac CTA image segmentation remains challenging due to the heterogeneity and complexity of cardiac CTA image data, and the lack of cardiac CTA images with annotations is also a major problem. Convolutional neural networks have been widely used as a deep learning method for segmentation of organs and pathological tissues in medical images. Christian F. Baumgartner et al.[7] studied the

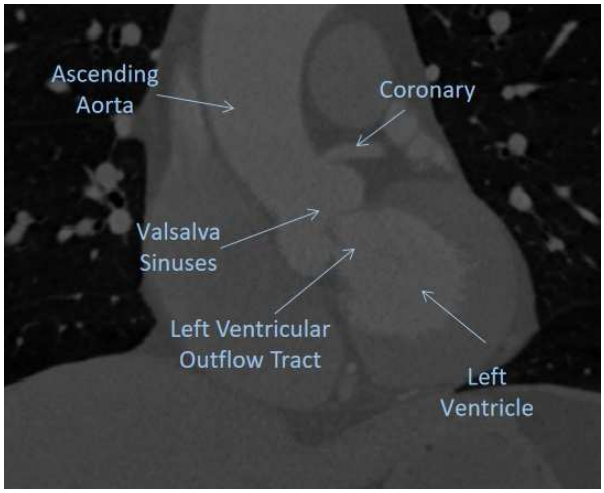

FIG. 1: Coronal view of a cardiac CT scan.

[a)]Author to whom correspondence should be addressed: hongzengxu@gmail.com

heart segmentation tasks of 2D CNNs and 3D CNNs, explored the use of a few parameters, and showed that using an optimized 2D CNN — produced better results than using a 3D CNN. Pablo G. Tahoces et al.[8] proposed a method based on pretrained CNN models that can effectively detect the aortic root. Duanduan Chen et al.[9] proposed a CNN based multistage segmentation framework that can effectively segment aortic dissection from CT images. Ronneberger et al.[10] proposed a new fully convolutional neural network U-net based on FCN[11], which is suitable for smaller datasets. The U-net network uses a skip connection to connect the downsampling layer and the upsampling layer, allowing the network to train fewer images but obtain better results. The U-net network performs very well in the field of medical image segmentation. As a result, many scholars have used the U-net network as the basic framework for medical segmentation tasks. Lohendran Baskaran et al.[12] used U-net to automatically segment multiple cardiovascular structures from cardiac CTA. In addition, 3D U-Net[13] is an improvement of 2D U-Net. Marija Habijan et al.[14] proposed a whole heart structure segmentation based on 3D U-Net combined with principal component analysis (PCA) as an additional data augmentation technique and discussed the effect of different learning rates on the final segmentation results. Although the abovementioned DL methods can generally obtain a better segmentation effect, for different subject data, it is necessary to manually adjust the model parameters in the preprocessing and postprocessing operations before training. As a result, the generalization performance of the model is low and cannot meet the needs of complex clinical applications.

The proposed model nnU-Net (no-new-Net)[15] is a DL network model applied to medical image segmentation tasks. The network is based on the U-Net structure, and the essential parts are preprocessing, training, inference strategies and postprocessing. The core idea is to automatically adjust the parameters in data preprocessing according to the characteristics of the different datasets that are input and to automatically adjust the hyperparameters in the training network according to the attributes of different training sets and computer devices. nnU-Net has demonstrated advanced performance in six recognized segmentation challenges and has been widely used. Such as caries detection and classification[16], segmentation of whole breast and fibroglandular tissue[17], COVID-19 CT lung and infection segmentation[18], and multiorgan abdominal CT segmentation[19]. However, to the best of our knowledge, nnU-Net has not been applied to the image segmentation task for preoperative simulation of cardiac aortic valve surgery.

Cardiac CTA mainly includes aortic vessels, coronary vessels, the left ventricle and other soft tissues. The purpose of our experiment was to provide an image reference for the preoperative simulation of aortic valve surgery. As a result, the aortic valve and nearby tissues are the segmentation objects that we focused on. As shown in Fig. 1, the aortic valve is at the root of the aorta and has a nearly spherical structure in appearance. Its upper part connects to the aorta, its lateral part connects to the coronary artery, and its lower part connects to the left ventricular outflow tract (the part of the left ventricle). Based on the above structure, the key parts of the image data (DICOM format) of the subject are extracted. The ground truth labeled images were generated by a thresholding operation by replacing the pixel values within the annotated area with 1 and the pixel values outside the annotated area with 0. The original and labeled images are converted from DICOM format (512×512 matrix) to NIFTI format (512×512 matrix), which are used for training and inference of the nnU-Net model.

Based on the classical U-shaped encoder-decoder architecture, nnU-Net performs data augmentation, image cropping, resampling, and data normalization operations based on image modality, voxel spacing, and resolution properties. Data augmentation uses rotation, scaling, gaussian noise, gaussian blur, brightness processing, contrast adjust, simulation of low-resolution, gamma augmentation and mirroring. An interpolation algorithm is used for resampling. The X and Y axis use the cubic spline interpolation method, and the Z axis use the nearest neighbor interpolation method. The CT value range of the pixels at the label position in the dataset was calculated, and the CT value was cropped in the range of 0.5% to 99.5% to normalize the image data. Image inference is through a sliding window. The size of the window is equal to the patch size during training. To suppress artifacts generated during the stitching process and reduce the influence of positions close to the image boundary, Gaussian importance weighting is used to suppress stitching artifacts. Taking cardiac CTA images with different image parameters as the research object, the model is trained, and the segmentation performance is evaluated. The segmentation results will be used in the preoperative simulation of TAVI.

I. MATERIAL PREPARATION

The cardiac CTA data of the subjects in this study is obtained from the Department of Cardiology, the People's Hospital of China Medical University and Key Laboratory of Cardiovascular Imaging and Research of Liaoning Province. Total 130 cases of 3D scanned cardiac data were collected from 2019 to 2021, including 88 cases in the training set, 22 cases in the validation set, and 20 cases in the test set. Subjects range in age from 44 to 82, with a mean age of 56.36. This study was approved by the Ethics Committee of the hospital, and informed consent was obtained from all individuals who participated in the study. The dataset consisted of general cases and cases of coronary and aortic vascular calcification and had different clinical imaging parameters. Information on the imaging acquisition parameters are shown in the TABLE I.

The dataset labels were semiautomatically segmented by the clinician using the ITK-SNAP[20] software . As shown in

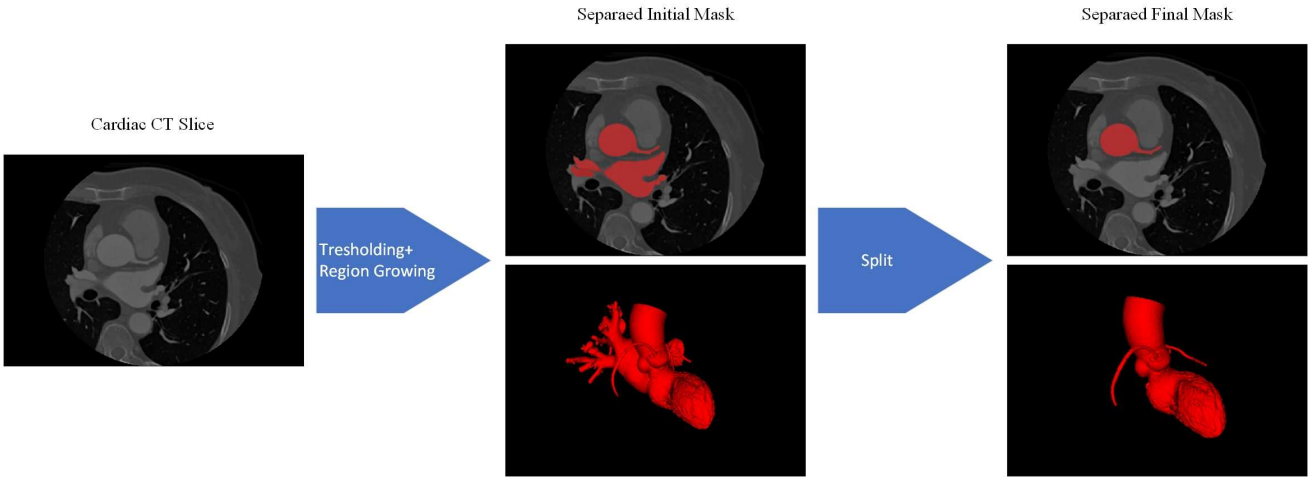

FIG. 2: The workflow of initial annotation by using ITK-SNAP.

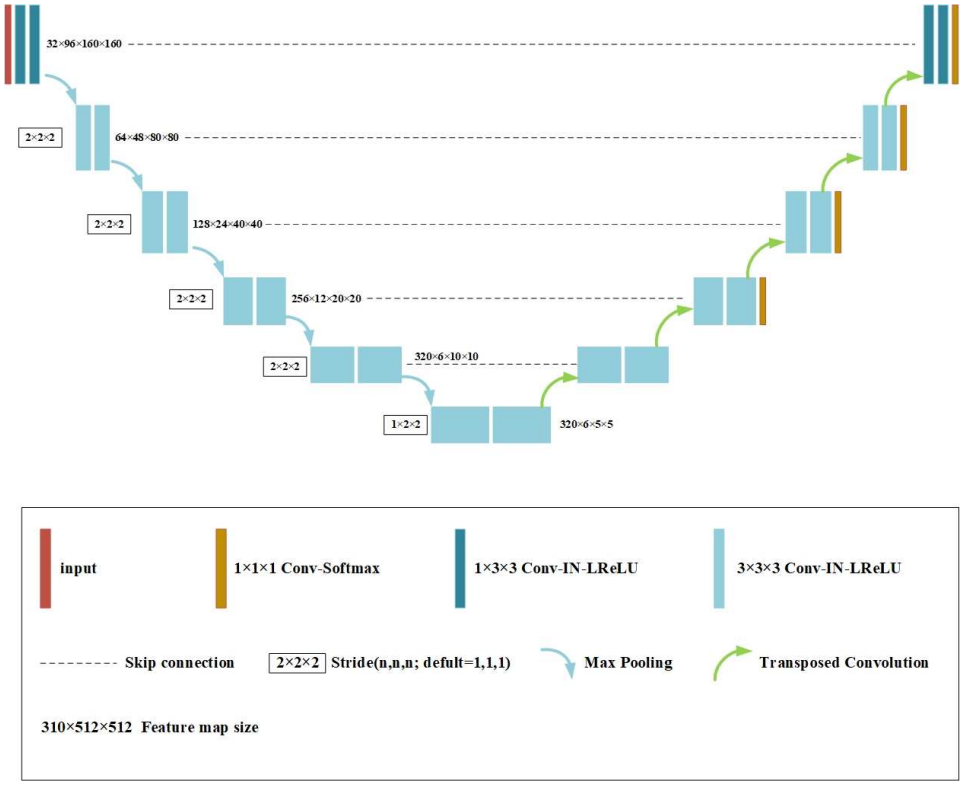

FIG. 3: The deep learning network architecture.

Fig. 2, the segmentation sites mainly included the aorta, the valsalva sinuses, the left and right proximal coronary arteries, and the left ventricle. The window width and window position were first adjusted to consider the region that contained the contrast, and then, the desired site was obtained by placing seed points and adjusting the growth range by the region growth algorithm to obtain the final segmentation result. The segmented images were examined by medical imaging specialists and the final result was identified as the correct labeling result of the training and verification (i.e., ground truth).

II. CARDIOVASCULAR SEGMENTATION NETWORK BASED ON NNU-NET

The main task of this research was to segment the aortic valve and nearby tissues. Here, nnU-Net was used as the Backbone. A 3D full resolution U-Net was automatically generated by nnU-Net for the cardiac CTA images. nnU-Net will preprocess the input data, and the nnU-Net network model would automatically generate the hyperparameters required for model training based on the preprocessed data and GPU

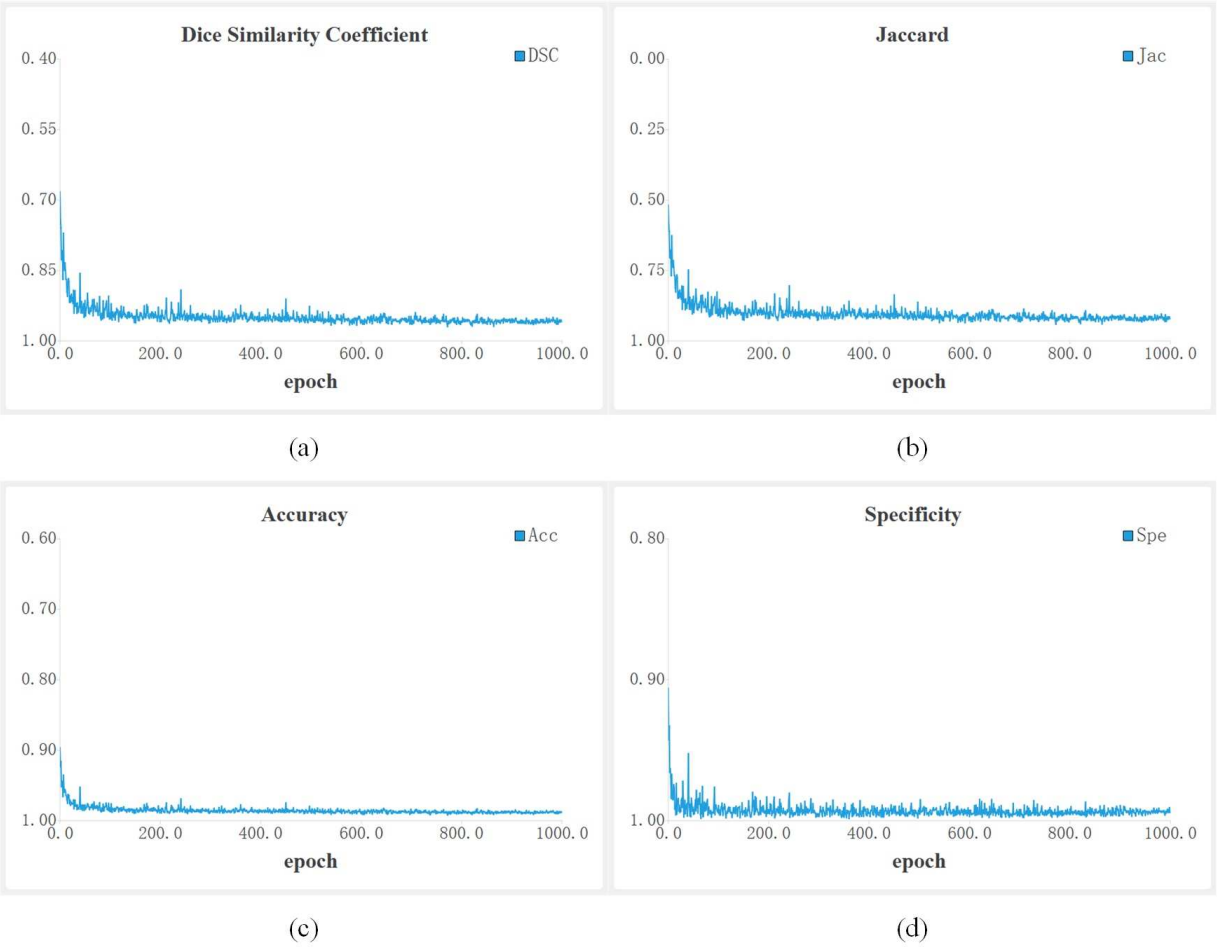

FIG. 4: Performance statistics of the model (DSC, Jac, Acc, Spe). Higher values of these four indicators indicate better results. (a) : Dice Similarity Coefficient, (b) : Jaccard, (c) : Accuracy and (d) : Specificity.

TABLE I: A summary infomation of the used datasets.

	LS[a]	VR[b] (X^e,Y^e)	VR (Z^e)	SR[c] (X,Y, (mm))	SR (Z, (mm))	TS[d]
Training set	88	512	212 ∼ 399	0.3301 ∼ 0.5957	0.44 ∼ 0.625	27210
Validation set	22	512	261 ∼ 399	0.3379 ∼ 0.5566	0.45 ∼ 0.625	6773
Test set	20	512	247 ∼ 356	0.4297 ∼ 0.5801	0.45	6576

[a] LS: Labeled scans.
[b] VR: Voxel range.
[c] SR: Spacing range.
[d] TS: Total slices
[e] X, Y, Z: Axis.

memory size. The patch is $96 \times 160 \times 160$ size and the minimum batch size was set to 2. As shown in Fig. 3, a U-shaped network linking the encoder path and decoder path by skip connection is trained for segmentation tasks. The convolutional block of each path contains two convolutional kernels of $2 \times 2 \times 2$ size. An instance normalization (IN) layer and a Leaky rectified linear unit (Lakey ReLU) are connected after the convolutional kernels. Downsampling uses max pooling with a $2 \times 2 \times 2$ size to reduce the image resolution, and the downsampling process ends with 320 feature maps of $4 \times 4 \times 4$ size, which are then recovered in size by the decoder path. The upsampling in the decoder path is implemented by $2 \times 2 \times 2$ size deconvolution, and the output segment map is obtained by softmax through the feature map and the $1 \times 1 \times 1$ size convolution kernel.

We combine the dice loss and cross-entropy loss to train the network. Dice loss is more suitable for data with heterogeneous samples. However, using dice loss has a bad effect on backpropagation, making the training unstable and the training error curve confusing, which makes it difficult to see the convergence information. The cross-entropy loss represents the distance between the actual output (probability) and the desired output (probability). In other words, the smaller the value of its result, the closer the two probability distributions, but cross-entropy only cares about the accuracy of the predicted probability for the correct label, ignoring the difference of the other incorrect labels, and thus, the learned features are

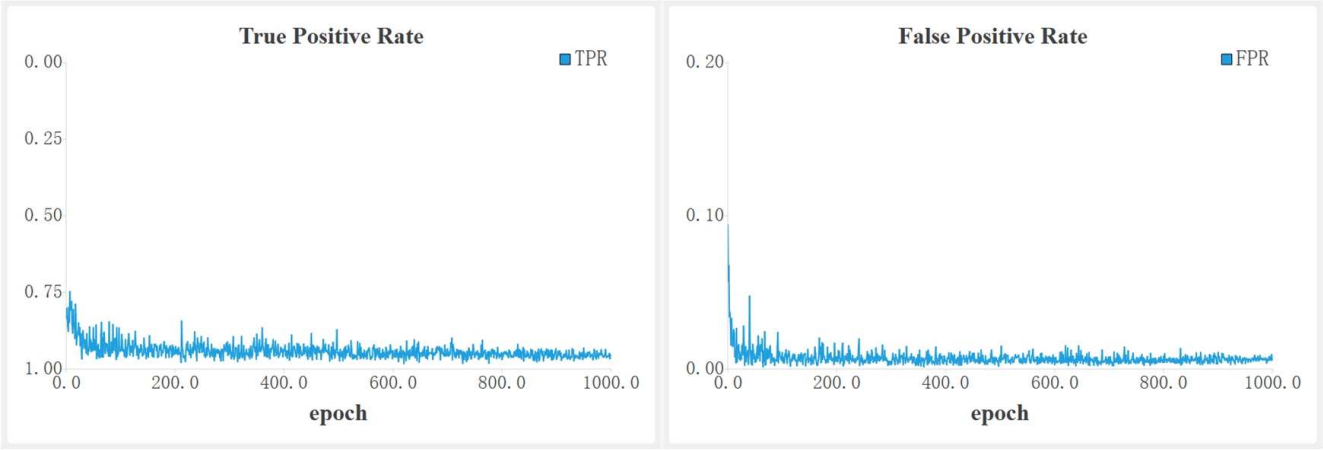

(a) (b)

FIG. 5: Performance statistics of model (TPR, FPR). (a) : True Positive Rate and (b) : False Positive Rate.

TABLE II: Summary of the results of validation set and test set used in nnU-Net model.

	Dice	Jac	Acc	Spe	TPR	FPR
Validation	0.9486±	0.9029±	0.9855±	0.9928±	0.9412±	0.0071±
set	0.0211	0.0343	0.0063	0.0053	0.0258	0.0053
Test	0.9698±	0.9414±	0.9989±	0.9994±	0.9731±	0.0006±
set	0.0081	0.0152	0.0004	0.0005	0.0223	0.0005

scattered. Therefore, the method of combining the two losses are chosen to improve the stability of the training and improve the accuracy of the segmentation. The loss function L_{Total} is determined as the sum of the dice loss L_{Dice} and cross entropy loss L_{CE}, and the formulas are as follows:

$$L_{\text{Total}} = L_{\text{Dice}} + L_{\text{CE}} \tag{1}$$

$$L_{\text{Dice}} = -\frac{2}{|K|}\sum_{k\in K}\frac{\sum_{n\in N} p_n^k y_n^k}{\sum_{n\in N} p_n^k + \sum_{n\in N} y_n^k} \tag{2}$$

$$L_{\text{CE}} = \frac{1}{N}\sum_{n\in N} -\left[y_n \cdot \ln(p_n) + (1-y_n)\cdot \ln(1-p_n)\right] \tag{3}$$

where K is the number of categories (K is 2 in this study), y is the one-hot encoding value, p is the softmax output probability, and N is the number of volume pixels in the training batch.

In this paper, based on the PyTorch platform, an SGD optimizer with Nesterov momentum set to 0.99 was selected , and the initial learning rate was set to 0.01. A total of 1000 epochs were trained, and each epoch was defined as the iterative optimization of 250 batches. Fivefold cross validation was used in the network training process to improve the generalization ability of the model. The experimental environment was an Intel (R) Xeon (R) CPU E5-2680 v4 @ 2.40 GHz×56, NVIDIA GeForce GTX 3070 8 GB, 188 GB running memory and Ubuntu 18.04.5 LTS operating system.

III. SEGMENTATION PERFORMANCE EVALUATION AND RESULTS

To verify the segmentation performance of the model, the experimental results can be further objectively evaluated. We use the Dice similarity coefficient (DSC), Jaccard coefficient (Jac), Accuracy (Acc), and Specificity (Spe) as indicators. The formulas of the above index are shown below. Where TP, FP, TN, and FN represent true positive, false positive, true negative and false negative, respectively.

$$\text{DSC} = \frac{2\times TP}{TP+FP+TP+FN} \tag{4}$$

$$\text{Jac} = \frac{TP}{TP+FP+TN} \tag{5}$$

$$\text{Acc} = \frac{TP+TN}{TP+TN+FP+FN} \tag{6}$$

$$\text{Spe} = \frac{TN}{TN+FP} \tag{7}$$

TABLE III: Dice values of our solution and other methods

Author	Method	Test set	Medical tissue segmentation area	Dice
Cheung et al.[21]	2D U-net	14	Aortic and coronary arteries	0.912
Alice et al.[22]	2D Multi-view integration	10	Aortic lumen	0.92± 0.001
Yu et al.[23]	3D U-net	25	Entire aorta	0.958
Ours	3D nnU-net	20	Aortic root and nearby tissues	0.9698± 0.0081

The performance statistics of the model relative to the validation set during training are given in Fig. 4. The metrics of the cardiac CTA aortic segmentation images obtained are relative to the validation set, and lead to better results in the test set. The comparison results are all shown as the mean ± standard in TABLE II

It can be seen from the performance metrics data that the four metrics of the model gradually smooth out and converge as the number of training rounds increases. Especially after 800 rounds of epoch training, the performance parameters of the model converge to a more stable result. However, the volume of the region of interest that we need to segment is relatively large compared with segmenting only the aorta and coronary arteries[21]. However, the segmentation results using this model are clearly not affected by the volume size of the segmented region and maintain an excellent and stable result overall from the final results. This finding shows that the DL method based on nnU-Net not only saves considerable time and ensures reliable accuracy compared with manual segmentation, but also has better generalization ability compared with other DL methods that require manual parameter adjustment.

For the evaluation of the performance of medical image segmentation models, there is usually a TPR (true positive rate) and an FPR (false positive rate). The formulas are as follows:

$$\text{TPR} = \frac{TP}{TP+FN} \tag{8}$$

$$\text{FPR} = \frac{FP}{FP+TN} \tag{9}$$

Medical images segmented by DL are prone to oversegmentation. In other words, they can generate excessive FPR. As shown in Fig. 5, The comparison results were all shown as mean ± standard in TABLE II. The result has a higher TPR and a lower FPR, which indicates that the model can maximize avoiding oversegmentation.

At present, the automated methods developed to process cardiac CTA images are still very few, and the majority of them dose not provide sufficient details to make comparison with our method due to the differences in the specific segmentation region. We could not make an objective comparison of segmentation accuracy based on various clinical datasets. In general, deep learning frameworks are superior to classical methods, and the results of our method have shown the advantage. We make the comparison between several deep learning methods. The Dice values reported in the literatures [21-23] are presented in TABLE III, and higher Dice scores can be obtained by our proposed method. In addition, our segmentation model was applied to Key Laboratory of Cardiovascular Imaging and Research of Liaoning Province, and its segmentation performed also very well.

In deep-learning-based methods, parameters need to be tuned accordingly when working with different datasets or exploring clinical applications. The nnU-Net method avoids complex and tedious parameter setting through adaptive preprocessing and postprocessing, as well as a robust training strategy. Therefore, integrating this method into the clinical application of TAVI can provide a good basis for subsequent research. To further evaluate the stability and performance of the nnU-Net method, more medical institution datasets to obtain a more robust model are required.

The cardiac CTA images of the subjects are shown from the axial view, sagittal view, coronal view, and 3D view, as shown in Fig. 6. The DL method using nnU-Net was evaluated on the cardiac CTA images of 20 subjects, and our inference results were compared with manually segmented pictures in different views, especially the key parts of the aorta, valsalva sinus, coronary arteries, and left ventricle. From the inferred images, a high degree of similarity to the labeled images was maintained overall, but the segmentation of the proximal coronary arteries were slightly shorter than the coronary artery part of the label. However, the proximal segmentation of the coronary arteries were slightly shorter relative to the labeled coronary portion, which did not have a significant impact on the segmentation metrics due to the small proportion of coronary volume in the overall picture. Our purpose in segmenting cardiac CTA images carrying a portion of the coronary artery was to assess the effect of cardiac valve stents on coronary port occlusion. As a result, the segmentation length of the coronary artery does not affect the actual preoperative simulation requirements.

The DL method based on nnU-Net can complete cardiac CTA image segmentation accurately and effectively on cardiac CTA datasets, and the predicted images have high agreement with the labeled images. Especially for the segmentation of the aorta and aortic valve and left ventricular outflow tract, no further manual repair is required. The ability to segment the aorta and the proximal border of the coronary artery, the left ventricle, and not too much soft tissue (e.g. pericardium, atrium) better indicates that the confidence of its segmentation results is high. As shown in Fig. 7, its segmentation results can be converted into stereolithography (STL) files for 3D printing surgical evaluation and hemodynamic analysis, which can be used as a reference for TAVI, which basically meets the requirements of preoperative simulation.

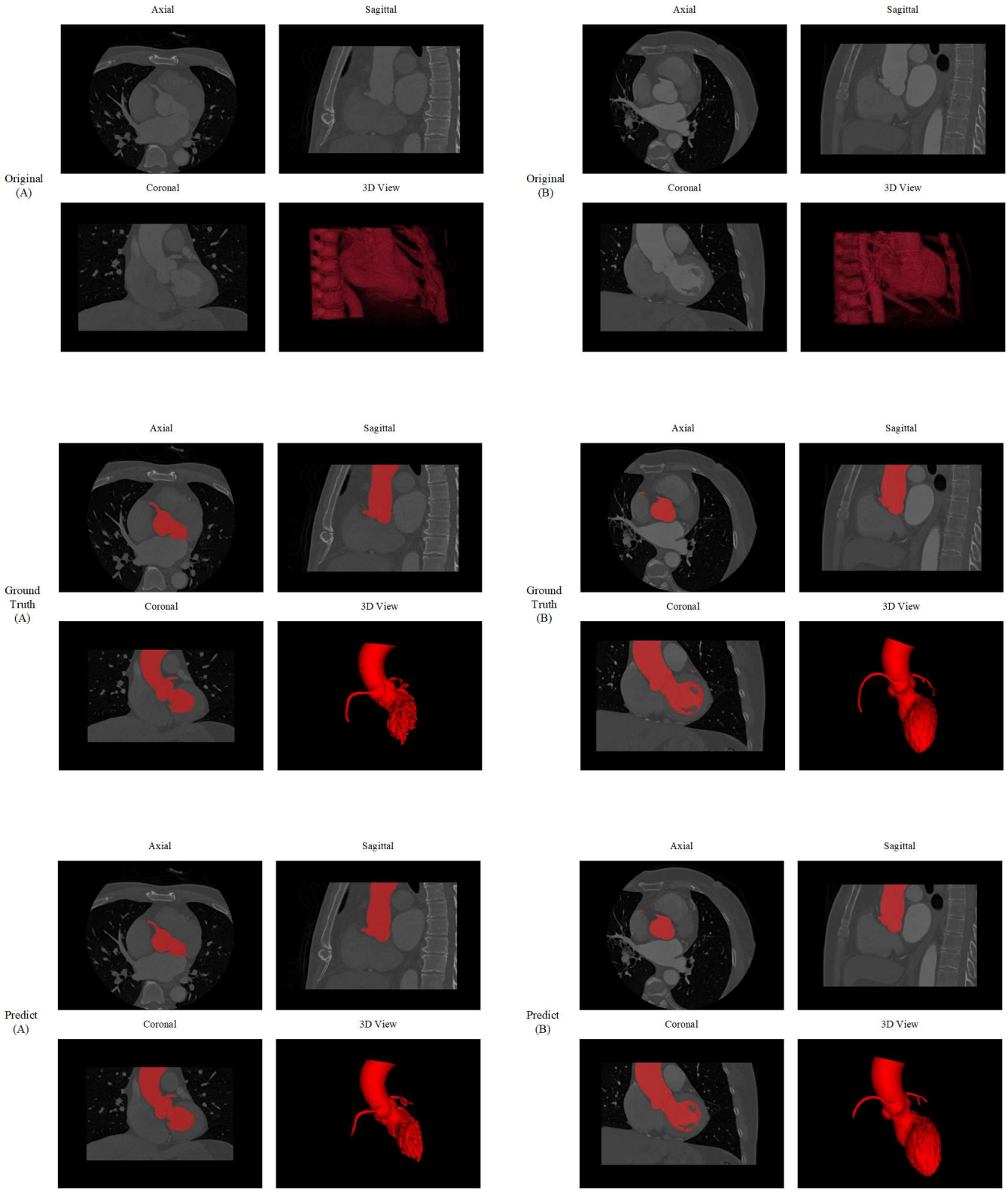

FIG. 6: The results of segmentation of representative cases with two different cardiac CTA imaging parameters using nnU-Net. The original image, ground truth image and prediction image of two cases (A,B) were compared from axial, sagittal, coronal and 3D view respectively. From top to down: original image, ground truth image and prediction image.

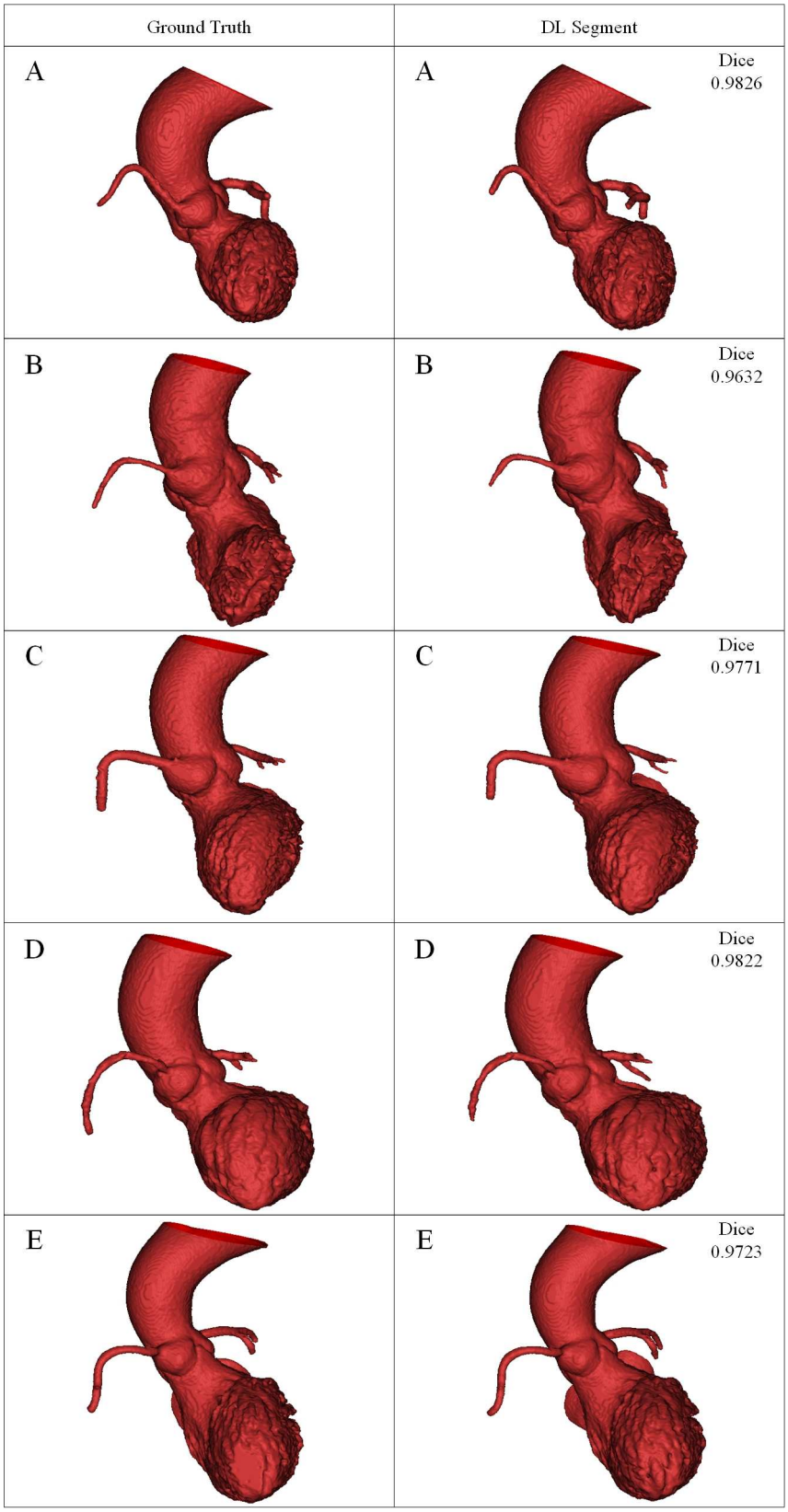

FIG. 7: The segmentation results of the cardiac CTA image is converted into STL files. These are the GT and DL segmentation results for five cases (A, B, C, D, E) and are displayed in 3D view by minics software. From the 3D view, the segmentation results had clear outline and vascular structures. Five cases with Dice of (A) 0.9826, (B) 0.9632, (C) 0.9771, (D) 0.9822 and (E) 0.9723.

IV. SUMMARIZES

In this paper, we studied the DL method based on nnU-Net for the segmentation of cardiac CTA images. and obtained a better DSC result of 0.9698 ± 0.0081 by training and testing the model on cardiac CTA image data with different parameters. The trained model was tested for inference and its results illustrate that the model can segment the valsalva sinusesand nearby cardiovascular system accurately and effectively. Compared with traditional methods, it not only ensures a high accuracy but also minimizes the impact of multiple types of patient data and image quality on the segmentation results. Compared with other DL methods, there is no need to manually adjust the network parameters, which is of high clinical application in processing cardiac CTA images and can provide powerful help for preoperative simulation of TAVI. In future work, we will continue to investigate the segmentation of the model in cardiac CTA images of patients with different degrees of aortic valve calcification, and will further improve the segmentation performance and shorten the segmentation time by increasing the training dataset and optimizing the model.

ACKNOWLEDGMENTS

The paper was supported by project of Shenzhen science and technology innovation committee (JCYJ20190809145407809, KJ2021C019). This research is also supported by the National Research Foundation, Singapore under its Strategic Capability Research Centres Funding Initiative. Any opinions, findings and conclusions or recommendations expressed in this material are those of the authors and do not reflect the views of National Research Foundation, Singapore.

[1]Z. Turani, R. A. Zoroofi, and S. Shirani, "3d automatic segmentation of coronary artery based on hierarchical region growing algorithm (3d hrg) in cta data- sets," in *2013 20th Iranian Conference on Biomedical Engineering (ICBME)* (2013) pp. 275–279.

[2]R. Latha and S. Senthilkumar, "Robust segmentation of blood vessels from angiographic images of the human heart," in *2010 International Conference on Communication and Computational Intelligence (INCOCCI)* (2010) pp. 174–177.

[3]Z. Turani, R. A. Zoroofi, S. Shirani, and S. Abkhofte, "Cardiovascular segmentation based on hough transform and heuristic knowledge," in *2012 19th Iranian Conference of Biomedical Engineering (ICBME)* (2012) pp. 309–312.

[4]F. Yang, Z.-G. Hou, S.-H. Mi, G.-B. Bian, and X.-L. Xie, "Segmentation and visualization of the heart region for 3-d simulation of coronary intervention procedures," in *Proceedings of the 33rd Chinese Control Conference* (2014) pp. 8408–8413.

[5]J.-W. Bai, P.-A. Li, and K.-H. Wang, "Automatic whole heart segmentation based on watershed and active contour model in ct images," in *2016 5th International Conference on Computer Science and Network Technology (ICCSNT)* (2016) pp. 741–744.

[6]J. Peters, O. Ecabert, C. Lorenz, J. V. Berg, M. J. Walker, T. B. Ivanc, M. Vembar, M. E. Olszewski, and J. Weese, "Segmentation of the heart and major vascular structures in cardiovascular ct images," Proceedings of Spie the International Society for Optical Engineering **6914** (2008), 10.1117/12.768494.

[7]C. F. Baumgartner, L. M. Koch, M. Pollefeys, and E. Konukoglu, "An exploration of 2d and 3d deep learning techniques for cardiac mr image segmentation," Springer, Cham , 111–119 (2017).

[8]P. G. Tahoces, R. Varela, and J. M. Carreira, "Deep learning method for aortic root detection," Computers in Biology and Medicine **135**, 104533 (2021).

[9]A. Dc, A. Xz, A. Ym, B. Fl, A. Hx, A. Zl, C. Qx, G. D. Wei, E. Hz, and A. Ty, "Multi-stage learning for segmentation of aortic dissections using a prior aortic anatomy simplification - sciencedirect," Medical Image Analysis **69**, 101931 (2021).

[10]O. Ronneberger, P. Fischer, and T. Brox, "U-net: Convolutional networks for biomedical image segmentation," Springer International Publishing , 234–241 (2015).

[11]J. Long, E. Shelhamer, and T. Darrell, "Fully convolutional networks for semantic segmentation," IEEE Transactions on Pattern Analysis and Machine Intelligence **39**, 640–651 (2015).

[12]L. Baskaran, S. J. Al'Aref, G. Maliakal, B. C. Lee, and L. J. Shaw, "Automatic segmentation of multiple cardiovascular structures from cardiac computed tomography angiography images using deep learning," PLoS ONE **15**, e0232573 (2020).

[13]z. iek, A. Abdulkadir, S. S. Lienkamp, T. Brox, and O. Ronneberger, "3d u-net: Learning dense volumetric segmentation from sparse annotation," Springer International Publishing , 424–432 (2016).

[14]M. Habijan, H. Leventić, I. Galić, and D. Babin, "Whole heart segmentation from ct images using 3d u-net architecture," in *2019 International Conference on Systems, Signals and Image Processing (IWSSIP)* (2019) pp. 121–126.

[15]F. Isensee, P. Jaeger, S. Kohl, J. Petersen, and K. Maier-Hein, "nnu-net: a self-configuring method for deep learning-based biomedical image segmentation," Nature Methods **18**, 1–9 (2021).

[16]L. Lian, T. Zhu, F. Zhu, and H. Zhu, "Deep learning for caries detection and classification," Diagnostics **11**, 1672 (2021).

[17]L. Huo, X. Hu, Q. Xiao, Y. Gu, X. Chu, and L. Jiang, "Segmentation of whole breast and fibroglandular tissue using nnu-net in dynamic contrast enhanced mr images," Magnetic Resonance Imaging **82**, 31–41 (2021).

[18]J. Ma, Y. Wang, X. An, C. Ge, Z. Yu, J. Chen, Q. Zhu, G. Dong, J. He, Z. He, *et al.*, "Toward data-efficient learning: A benchmark for covid-19 ct lung and infection segmentation," Medical physics **48**, 1197–1210 (2021).

[19]G. Zhang, Z. Yang, B. Huo, S. Chai, and S. Jiang, "Multiorgan segmentation from partially labeled datasets with conditional nnu-net," Computers in Biology and Medicine **136**, 104658 (2021).

[20]P. A. Yushkevich, J. Piven, H. C. Hazlett, R. G. Smith, S. Ho, J. C. Gee, and G. Gerig, "User-guided 3d active contour segmentation of anatomical structures: Significantly improved efficiency and reliability," NeuroImage **31**, 1116–1128 (2006).

[21]W. K. Cheung, R. Bell, A. Nair, L. J. Menezes, and J. Jacob, "A computationally efficient approach to segmentation of the aorta and coronary arteries using deep learning," IEEE Access **PP**, 1–1 (2021).

[22]F. A, E. M, F. A, A. F, P. B, B. C, S. G, and C. M., "3d automatic segmentation of aortic computed tomography angiography combining multi-view 2d convolutional neural networks," Cardiovascular engineering and technology **11**, 576–586 (2020).

[23]Y. Yu, Y. Gao, J. Wei, F. Liao, Q. Xiao, J. Zhang, W. Yin, and B. Lu, "A three-dimensional deep convolutional neural network for automatic segmentation and diameter measurement of type b aortic dissection." The Korean Society of Radiology **22**, 168–178 (2021).